

Mussel-Inspired Chemistry and Michael Addition Reaction for Efficient Oil/Water Separation

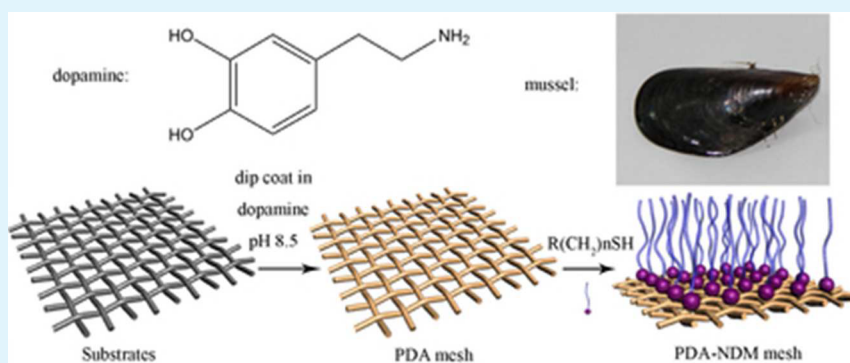
Yingze Cao,[†] Xiaoyong Zhang,[†] Lei Tao,[†] Kan Li,[§] Zhongxin Xue,[§] Lin Feng,^{*,†} and Yen Wei^{*,†,‡}

[†]Department of Chemistry, Tsinghua University, Beijing 100084, P. R. China

[‡]Key Lab of Organic Optoelectronic & Molecular Engineering of Ministry of Education, Department of Chemistry, Tsinghua University, Beijing 100084, P. R. China

[§]Institute of Chemistry, Chinese Academy of Sciences, Beijing 100190, P. R. China

S Supporting Information



ABSTRACT: An oil/water separation mesh with high separation efficiency and intrusion pressure of water has been successfully developed by combining mussel-inspired chemistry and Michael addition reaction. The substrate of the stainless steel mesh was first coated with the adhesive polydopamine (PDA) film by simple immersion in an aqueous solution of dopamine at pH of 8.5. Then n-dodecyl mercaptan (NDM) was conjugated with PDA film through Michael addition reaction at ambient temperature. The as-prepared mesh showed highly hydrophobicity with the water contact angle of 144° and superoleophilicity with the oil contact angle of 0°. It can be used to separate a series of oil/water mixtures like gasoline, diesel, etc. The separation efficiency remains high after 30 times use (99.95% for hexane/water mixture). More importantly, the relatively high intrusion pressure (2.2 kPa) gives the opportunity to separation of large amount of oil and water mixtures. This study provides a new prospect to simply introduce multiple molecules on the adhesive PDA-based mesh to achieve various functional oil/water separation materials.

KEYWORDS: mussel-inspired chemistry, Michael addition reaction, highly hydrophobic, superoleophilic, nanostructured, oil/water separation

1. INTRODUCTION

Oil/water separation has attracted considerable attention due to the serious water pollution like oil spill accidents, oily wastewater from industries, etc. Thus, materials that can effectively separate water and oil are in urgent demand.^{1–7} The wettability of solid surface is very important which can be used to design such materials. Chemical composition and the geometrical microstructure are two main factors that affect the wettability.^{8–17} In the past decade, much research has focused on developing surfaces with both superhydrophobicity and superoleophilicity, which can effectively separate the mixture of oil and water. Generally, the majority studies put emphasis on two aspects. One is modifying meshes with low surface energy substances such as fluorochemicals.^{18–21} The other is fabricating meshes with hierarchical microstructure and nanostructure surface though corrosion, electro-deposition, and so on.^{22–28} However, it is still a challenge to obtain superhydrophobic and superoleophilic meshes by using

environmentally friendly and low cost chemicals as well as under simple and easy conditions.

Inspired by the strong adhesive protein in mussels, dopamine is chosen as a molecular structural mimic of the *Mytilus edulis* foot protein 5 (Mefp-5). Messersmith and co-workers have confirmed in their early work that dopamine through self-polymerization can form strong covalent and noncovalent interactions with virtually all types of inorganic and organic substances.^{29–32} Recently, the Haeshin Lee group found that polydopamine is considered to be formed cocontribution of noncovalent self-assembly and covalent polymerization.³³ The study has been widely applied in many fields like surface coating, immobilization of peptides and molecules, medical adhesive, and encapsulation.^{34–40} Reverse osmosis membranes

Received: March 7, 2013

Accepted: April 18, 2013

Published: April 18, 2013

have also been surfaced-modified with polydopamine. The membranes with nanopores showed underwater superoleophobicity that are resistant to salt and organic molecules.⁴¹ Apart from the attractive adhesion property of dopamine, it also has made great contribution to obtaining surfaces with high active reaction sites by simple dip-coating of objects in an aqueous solution of dopamine. Functional multilayer films have been fabricated by the integration of mussel-inspired catechol oxidative chemistry into layer-by-layer assembly. The surface wettability of films has been studied, and the water contact angle after modifying thiols is about 60°.⁴² The polydopamine coated surfaces as a platform for secondary reaction with thiol or amino group through Michael addition reaction make it possible for various molecules to be introduced into the surfaces.⁴³ Therefore, mussel-inspired chemistry has a great opportunity to develop inexpensive, bearable for a large amount of oil and water, efficient, and reusable oil/water separation materials in a friendly environment.

In this work, a novel and facile method by combining mussel-inspired chemistry and Michael addition reaction to prepare efficient oil/water separation mesh films has been developed. The stainless steel mesh was first coated with the adhesive film by immersion in an aqueous solution of dopamine at pH of 8.5. N-Dodecyl mercaptan (NDM) was conjugated with PDA film through the Michael addition reaction afterward (Figure 1).

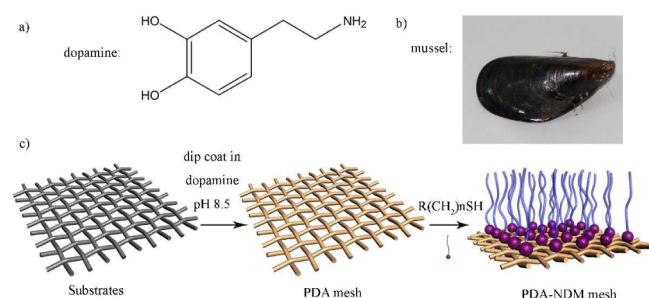


Figure 1. a) Chemical structure of dopamine; b) photograph of a mussel; c) schematic description of the preparation of polydopamine coated stainless steel mesh film and N-dodecyl mercaptan modified surface through Michael addition reaction.

The as-prepared PDA-NDM mesh is highly hydrophobic and superoleophilic, which can be used effectively for a large amount of oil/water separation. The separation efficiency remains high after 30 times use and can be easily cleaned and stored. Hence, it has given a brand new method to modify the mesh in a straightforward and friendly way. Other functional molecules with hydrophilic and responsive groups can be expected to introduce on the mesh to achieve various oil/water separation meshes.

2. EXPERIMENTAL SECTION

2.1. Materials and Measurements. Dopamine hydrochloride (Sangon Biotech Co. Ltd., Shanghai, China) and n-dodecyl mercaptan (Aladdin Industrial Inc., Shanghai, China) were used as purchased. Other reagents from Sinopharm Chemical Reagents are of analytical grade and used without further purification.

2.2. Preparation of the PDA Mesh. The stainless steel mesh used as substrate was cleaned by ethanol and acetone. The mesh was cut into 4×4 cm² pieces and immersed in 60 mL of tris(hydroxymethyl) aminomethane solution (10 mmol/L, pH = 8.5). Then 120 mg of dopamine was added, and the mixture was placed at ambient temperature for 40 h. The PDA mesh was washed by deionized water and dried out for secondary reaction.

2.3. Preparation of the PDA-NDM Mesh. To obtain the PDA-NDM mesh, the PDA mesh was first immersed in 60 mL of NaOH solution (pH > 12). Second, 100 μ L of NDM was added into the mixture and reacted for 6 h at ambient temperature. The PDA-NDM mesh was cleaned by ethanol and diethyl ether twice for further characterization.

2.4. Characterization. The SEM images were obtained by a field-emission scanning electron microscope Hitachi S-4800 operated at 5.0 kV. The X-ray photoelectron spectra (XPS) were acquired by a VGESCALAB 220-IXL spectrometer using an Al K α X-ray source (1484.6 eV). Contact angles were measured on an OCA20 machine (Data-Physics, Germany) at ambient temperature. The average value of five measurements performed at different positions on the same sample was adopted as the contact angle.

Oil/water separation experiment of the PDA-NDM mesh: the as-prepared mesh was fixed between two Teflon fixtures. Both of the fixtures were attached with a glass tube and placed with a tilt angle of 15°. The diameter of the glass tube was 30 mm. The oil/water mixtures (50 v/v%) were poured onto the mesh. The separation was achieved by the force of gravity.

3. RESULTS AND DISCUSSIONS

3.1. Mesh Morphology. The SEM images of the substrate, the PDA mesh, and the PDA-NDM mesh are shown in Figure 2a-c, respectively. Figure 2a is a typical image of stainless steel

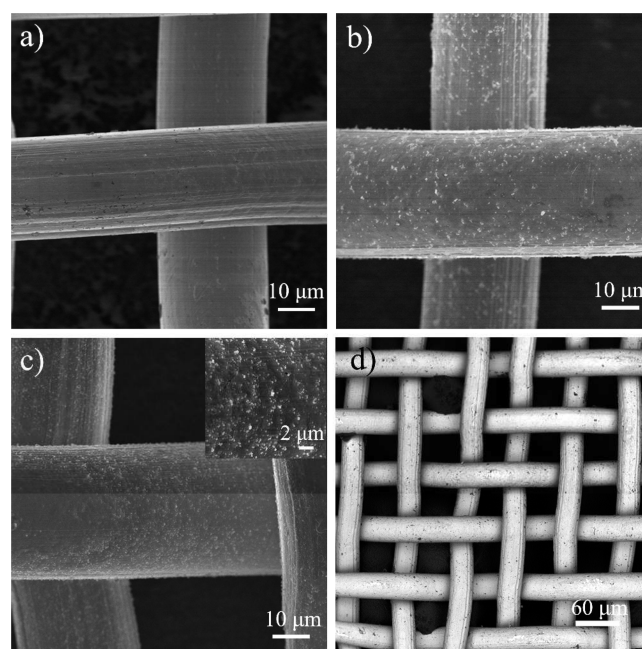


Figure 2. SEM images of the as-prepared mesh: a) the stainless steel mesh as substrates before coating of polydopamine; b) the polydopamine coated mesh showing rough surface with interval nanostructured papillae; c) more nanostructured papillae can be observed after conjugation between n-dodecyl mercaptan and the PDA mesh; the inset is a high-magnification of the PDA-NDM mesh. d) The low-magnification view of the PDA-NDM mesh with an average diameter of approximately 40 μ m.

substrate that is knitted by stainless steel wires with pore diameter of approximately 40 μ m. The uncoated mesh has a smooth and clear surface, while the PDA mesh has numerous nanostructured papillae on it (Figure 2b). Figure 2c is the image of the PDA-NDM mesh, and the inset demonstrates the nanostructured papillae get more intensive after the conjugation between n-dodecyl mercaptan and the PDA mesh. The roughness together with the property of n-dodecyl

mercaptan brings about the highly hydrophobicity, while the chemical affinity of n-dodecyl mercaptan ensure its superoleophilicity. Figure 2d shows low-magnification view of the PDA-NDM mesh with an average diameter of approximately 40 μm . With these holes on the mesh, oil can easily flow through the mesh.

3.2. Chemical Composition of the Mesh. Chemical composition of the substrate and coated mesh has been measured by XPS to further confirm the successful modification. The basic elements including carbon (C), oxygen (O), nitrogen (N), and sulfur (S) was surveyed by scanning bonding energy from 0 to 1200 eV (Figure 3a). The four main

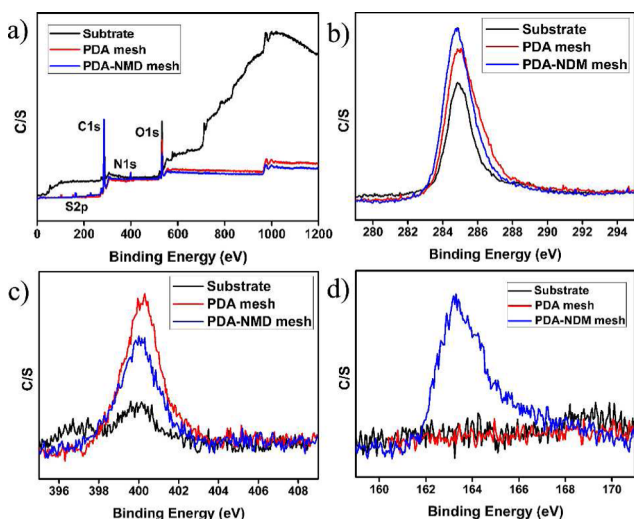


Figure 3. XPS spectra of the as-prepared mesh: a) survey scans the spectral region from 0 to 1200 eV; b-d) high-resolution XPS C1s, N1s, and S2p narrow scans as a function of electron binding energy (BE): the content of C gradually increased after each step; the increase of N content after dopamine self-polymerization and decrease after n-dodecyl mercaptan conjugation; sulfur element was first observed on the PDA-NDM mesh.

peaks at 171.0, 284.9, 400.1, and 532.7 eV have been labeled in Figure 3a and separately represent S2p, C1s, N1s, and O1s. The hump at 1000 eV was probably caused by the metallic elements on the substrates. In the spectrum of C1s (Figure 3b), the peak at 284.9 eV originate from sp^3 -hybridized carbon atoms (C–C). From Table 1, 2.5% Si was found on the PDA-mesh while 3.65% on the substrates, which means the results on the PDA-mesh column include both a small layer of the substrates and PDA films since dopamine does not contain Si. It also indicates that the C content of PDA films should be much higher than 74.68%. Similarly, the C content of the PDA-NDM mesh is the average value of the PDA film and the NDM film since

Table 1. Element Contents of the Substrates, the PDA Mesh, and the PDA-NDM Mesh Based on XPS Analysis

	substrates	PDA mesh	PDA-NDM mesh
C1s	56.07	74.68	77.18
N1s	2.49	5.44	4.1
O1s	31.73	17.37	12.94
S2p	0	0	2.87
Si2p	3.65	2.5	0
Fe2p3	4.02	0	0
Cr2p	2.04	0	0

dopamine contains nitrogen while NDM does not. Therefore, the carbon element content of the PDA-NDM mesh (77.18%) is larger than N-dodecyl mercaptan (calculated as 71.20%). Compared to the substrate, the N content of the PDA mesh was increased by 2.95%, and the metallic element can no longer be detected on the surface. Figure 3c illustrates the increase of N content after dopamine self-polymerization and the decrease after n-dodecyl mercaptan conjugation. Sulfur element was first observed on the PDA-NDM mesh in the high resolution spectra of S2p (Figure 3d), suggesting the linkage between n-dodecyl mercaptan and the PDA mesh.

3.3. Mesh Performance. The surface wettability of the PDA-NDM mesh has been characterized by the water contact angle measurement. Figure 4a displays the shape of a water

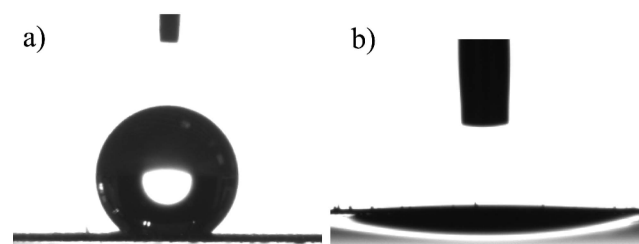


Figure 4. The as-prepared mesh shows special wettability: a) the photograph of a water droplet (2 μL) on the PDA-NDM mesh with a contact angle of $143.8 \pm 1.0^\circ$; b) a diesel oil droplet (2 μL) spread and permeate quickly on the mesh.

droplet on the as-prepared mesh, and in this case the water contact angle (WCA) is about $143.8 \pm 1.0^\circ$. Figure 4b illustrates the wetting and permeating behavior of diesel oil droplet on the mesh. In contrast, the oil contact angle (OCA) is close to 0° : the diesel oil can quickly spread and permeate the mesh. The opposite wettability: highly hydrophobicity and superoleophilicity of the PDA-NDM mesh results in the capacity of oil/water separation.

3.4. Separation of Oil and Water. A series of proof-of-concept studies were carried out to test the PDA-NDM mesh. The oil/water separation experiment procedure was performed as shown in Figure 5a, b. The mesh was fixed between two Teflon fixtures. Both of the fixtures were attached with glass tubes and placed with a tilt angle of 15° . Since the density of the tested oil hexane in this case is lighter than water, hexane will stay above water. The device was placed tilted so that hexane can have a contact with the mesh. As pouring the mixture of hexane (dyed by oil red) and water, hexane passed through the mesh quickly with the driving force of gravity, while water was repelled and kept in the upper glass tube (see details in the Supporting Information video). Mixtures of petroleum ether/water, gasoline/water, and diesel/water were also successfully separated with high efficiency. Almost no visible oil existed in the water after the separation, and the content of oil was measured using the infrared spectrometer oil content analyzer. The separation efficiency was calculated by the oil rejection coefficient (R (%)) according to

$$R(\%) = \left(1 - \frac{C_p}{C_0} \right) \times 100 \quad (1)$$

where C_0 and C_p are the oil concentration of the original oil/water mixtures and the collected water after the first separation. The separation efficiency of the PDA-NDM mesh for a series of

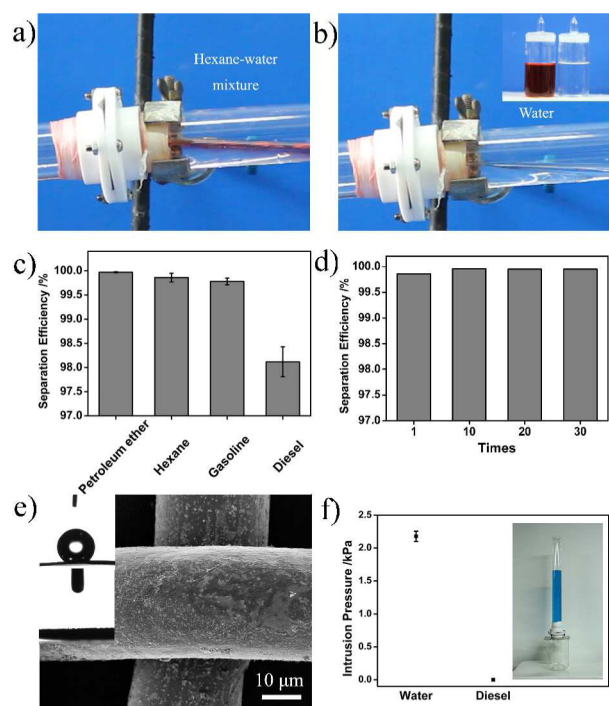


Figure 5. The studies of the PDA-NDM mesh. a) The mesh was fixed between two Teflon fixtures. Both of the fixtures were attached with glass tubes and placed with a tilt angle of 15°. A mixture of hexane and water was poured into the upper glass tube. b) Hexane passed through the mesh quickly, while the water was kept in the upper glass. After the separation, water and oil were collected, respectively. c) The separation efficiency of the PDA-NMD mesh for a selection of oil and water. d) Separation efficiency remains high after 30 times use by taking hexane as an example. e) Surface morphology has no change after use. The inset illustrates the shape of a water (above) and a diesel oil (below) droplet on the mesh after 30 times use. f) The intrusion pressure of water and diesel.

oils is above 99.7% except for diesel, as shown in Figure 5c. The separation efficiency of diesel ($98.12 \pm 0.31\%$) is a little lower than the others probably due to the diesel's complex composition and high viscosity. In addition, the as-prepared meshes can be easily cleaned and stored for reuse. The meshes maintain the high separation efficiency after 30 times use by taking the hexane/water mixture as an example (Figure 5d) as well the surface morphology of the mesh has not been destroyed (Figure 5e). The inset in Figure 5e illustrates that the surface of the mesh maintain highly hydrophobicity and superoleophilicity after 30 times use, showing its stable wettability.

Intrusion pressure is another evaluation for the oil/water separation mesh. The maximum height of water that the PDA-NDM mesh can support determined the intrusion pressure of water. The weight of water is also involved; therefore, the experimental intrusion pressure (P_{exp}) values were calculated by the following equation

$$P_{\text{exp}} = \rho gh_{\text{max}} \quad (2)$$

where ρ is the density of water, g is acceleration of gravity, and h_{max} is the maximum height of water the mesh can support. As shown in Figure 5f, the average intrusion pressure of five measurements is 2.18 ± 0.08 kPa, and the maximum bearable height achieved is 22.27 ± 0.87 cm. The intrusion pressure is relatively high compared to the earlier reports that illustrates

the stability of the as-prepared mesh.^{9,44} Water cannot flow through the mesh under the pressure. The intrusion pressures of oils are 0. Consequently, the as-prepared mesh is capable of separating a large amount of oil/water mixtures.

4. CONCLUSIONS

In summary, an oil/water separation mesh has been successfully fabricated by combining mussel-surface chemistry and Michael addition reaction. The PDA-NDM mesh can selectively separate water from oil/water mixtures with high efficiency, and they can be easily cleaned, stored, and reused. This separation material with high intrusion pressure gives the opportunity for separation of a large amount of oil/water mixtures. Furthermore, this study opens up a new application of mussel-inspired chemistry, and also we can introduce multitudinous functional molecules by employing the polydopamine coating process. Responsible materials for controllable oil/water separation can also be realized by means of simultaneously conjugating two kinds of substances with different wettability with the polydopamine coated mesh.

■ ASSOCIATED CONTENT

Supporting Information

Video of separation process by taking water and hexane mixtures as an example. This material is available free of charge via the Internet at <http://pubs.acs.org>.

■ AUTHOR INFORMATION

Corresponding Author

*E-mail: fl@mail.tsinghua.edu.cn (L.F.); weiyen@tsinghua.edu.cn (Y.W.).

Notes

The authors declare no competing financial interest.

■ ACKNOWLEDGMENTS

The authors are grateful for financial support from the National Natural Science Foundation (51173099, 21134004) and the National Research Fund for Fundamental Key Projects (2009CB930602 and 2011CB935700).

■ REFERENCES

- (1) Yuan, J.; Liu, X.; Akbulut, O.; Hu, J.; Suib, S. L.; Kong, J.; Stellacci, F. *Nat. Nanotechnol.* **2008**, *3*, 332–336.
- (2) Gui, X.; Wei, J.; Wang, K.; Cao, A.; Zhu, H.; Jia, Y.; Shu, Q.; Wu, D. *Adv. Mater.* **2009**, *22*, 617–621.
- (3) Feng, L.; Zhang, Z.; Mai, Z.; Ma, Y.; Liu, B.; Jiang, L.; Zhu, D. *Angew. Chem., Int. Ed.* **2004**, *43*, 2012–2014.
- (4) Zhang, L.; Zhang, Z.; Wang, P. *NPG Asia Mater.* **2012**, *4*, e8.
- (5) Qing, G.; Sun, T. *Adv. Mater.* **2011**, *23*, 1615–1620.
- (6) Sun, T.; Qing, G. *Adv. Mater.* **2011**, *23*, H57–H77.
- (7) Qing, G.; Wang, X.; Fuchs, H.; Sun, T. *J. Am. Chem. Soc.* **2009**, *131*, 8370–8371.
- (8) Drellich, J.; Chibowski, E.; Meng, D. D.; Terpilowski, K. *Soft Matter* **2011**, *7*, 9804–9828.
- (9) Xue, Z.; Wang, S.; Lin, L.; Chen, L.; Liu, M.; Feng, L.; Jiang, L. *Adv. Mater.* **2011**, *23*, 4270–4273.
- (10) Li, A.; Sun, H.-X.; Tan, D.-Z.; Fan, W.-J.; Wen, S.-H.; Qing, X.-J.; Li, G.-X.; Li, S.-Y.; Deng, W.-Q. *Energy Environ. Sci.* **2011**, *4*, 2062–2065.
- (11) Zhu, X.; Zhang, Z.; Ren, G.; Yang, J.; Wang, K.; Xu, X.; Men, X.; Zhou, X. *J. Mater. Chem.* **2012**, *22*, 20146–20148.
- (12) Kota, A. K.; Kwon, G.; Choi, W.; Mabry, J. M.; Tuteja, A. *Nat. Commun.* **2012**, *3*, 1025–1030.
- (13) Callies, M.; Quéré, D. *Soft Matter* **2005**, *1*, 55–61.

- (14) Shannon, M. A.; Bohn, P. W.; Elimelech, M.; Georgiadis, J. G.; Mariñas, B. J.; Mayes, A. M. *Nature* **2008**, *452*, 301–310.
- (15) Nordvik, A. B.; Simmons, J. L.; Bitting, K. R.; Lewis, A.; Ström-Kristiansen, T. *Spill Sci. Technol. Bull.* **1996**, *3*, 107–122.
- (16) Guix, M.; Orozco, J.; García, M.; Gao, W.; Sattayasamitsathit, S.; Merkoçi, A.; Escarpa, A.; Wang, J. *ACS Nano* **2012**, *6*, 4445–4451.
- (17) Korhonen, J. T.; Kettunen, M.; Ras, R. H.; Ikkala, O. *ACS Appl. Mater. Interfaces* **2011**, *3*, 1813–1816.
- (18) Yabu, H.; Shimomura, M. *Chem. Mater.* **2005**, *17*, 5231–5234.
- (19) Xie, Q.; Xu, J.; Feng, L.; Jiang, L.; Tang, W.; Luo, X.; Han, C. C. *Adv. Mater.* **2004**, *16*, 302–305.
- (20) Wang, Q.; Cui, Z.; Xiao, Y.; Chen, Q. *Appl. Surf. Sci.* **2007**, *253*, 9054–9060.
- (21) Shang, Y.; Si, Y.; Raza, A.; Yang, L.; Mao, X.; Ding, B.; Yu, J. *Nanoscale* **2012**, *4*, 7847–7854.
- (22) Feng, L.; Li, S.; Li, Y.; Li, H.; Zhang, L.; Zhai, J.; Song, Y.; Liu, B.; Jiang, L.; Zhu, D. *Adv. Mater.* **2002**, *14*, 1857–1860.
- (23) Wang, S.; Song, Y.; Jiang, L. *Nanotechnology* **2006**, *18*, 015103.
- (24) Li, M.; Xu, J.; Lu, Q. *J. Mater. Chem.* **2007**, *17*, 4772–4776.
- (25) Wang, C.; Yao, T.; Wu, J.; Ma, C.; Fan, Z.; Wang, Z.; Cheng, Y.; Lin, Q.; Yang, B. *ACS Appl. Mater. Interfaces* **2009**, *1*, 2613–2617.
- (26) Nguyen, D.-D.; Tai, N.-H.; Lee, S.; Kuo, W. *Energy. Environ. Sci.* **2012**, *5*, 7908–7912.
- (27) Wu, J.; Chen, J.; Qasim, K.; Xia, J.; Lei, W.; Wang, B.-p. *J. Chem. Technol. Biotechnol.* **2012**, *87*, 427–430.
- (28) Sato, O.; Kubo, S.; Gu, Z.-Z. *Acc. Chem. Res.* **2008**, *42*, 1–10.
- (29) Lee, H.; Dellatore, S. M.; Miller, W. M.; Messersmith, P. B. *Science* **2007**, *318*, 426–430.
- (30) Lee, H.; Rho, J.; Messersmith, P. B. *Adv. Mater.* **2008**, *21*, 431–434.
- (31) Kang, S. M.; Rho, J.; Choi, I. S.; Messersmith, P. B.; Lee, H. *J. Am. Chem. Soc.* **2009**, *131*, 13224.
- (32) Lee, H.; Lee, B. P.; Messersmith, P. B. *Nature* **2007**, *448*, 338–341.
- (33) Hong, S.; Na, Y. S.; Choi, S.; Song, I. T.; Kim, W. Y.; Lee, H. *Adv. Funct. Mater.* **2012**, *22*, 4711–4717.
- (34) Zhang, L.; Wu, J.; Wang, Y.; Long, Y.; Zhao, N.; Xu, J. *J. Am. Chem. Soc.* **2012**, *134*, 9879–9881.
- (35) Hu, H.; Yu, B.; Ye, Q.; Gu, Y.; Zhou, F. *Carbon* **2010**, *48*, 2347–2353.
- (36) Yu, B.; Wang, D. A.; Ye, Q.; Zhou, F.; Liu, W. *Chem. Commun.* **2009**, *44*, 6789–6791.
- (37) Yang, S. H.; Kang, S. M.; Lee, K.-B.; Chung, T. D.; Lee, H.; Choi, I. S. *J. Am. Chem. Soc.* **2011**, *133*, 2795–2797.
- (38) Ye, Q.; Zhou, F.; Liu, W. *Chem. Soc. Rev.* **2011**, *40*, 4244–4258.
- (39) Yang, K.; Lee, J. S.; Kim, J.; Lee, Y. B.; Shin, H.; Um, S. H.; Kim, J. B.; Park, K. I.; Lee, H.; Cho, S.-W. *Biomaterials* **2012**, *33*, 6952–6964.
- (40) Kang, S. M.; Hwang, N. S.; Yeom, J.; Park, S. Y.; Messersmith, P. B.; Choi, I. S.; Langer, R.; Anderson, D. G.; Lee, H. *Adv. Funct. Mater.* **2012**, *22*, 2949–2955.
- (41) Kasemset, S.; Lee, A.; Miller, D. J.; Freeman, B. D.; Sharma, M. *M. J. Membr. Sci.* **2013**, *425–426*, 208–216.
- (42) Wu, J.; Zhang, L.; Wang, Y.; Long, Y.; Gao, H.; Zhang, X.; Zhao, N.; Cai, Y.; Xu, J. *Langmuir* **2011**, *27*, 13684–13691.
- (43) Zhang, X.; Liu, M.; Zhang, Y.; Yang, B.; Ji, Y.; Feng, L.; Tao, L.; Li, S.; Wei, Y. *RSC Adv.* **2012**, *2*, 12153–12155.
- (44) Lee, C.; Baik, S. *Carbon* **2010**, *48*, 2192–2197.